

PROCEEDINGS, INDONESIAN PETROLEUM ASSOCIATION
Forty-Third Annual Convention & Exhibition, September 2019

**APPLICATION OF FULL WAVEFORM INVERSION TO RESOLVE AN ERODED SHALLOW
CARBONATE PLATFORM, NORTH MADURA, EAST JAVA, INDONESIA**

David Cavalin*
Nurrul Ismail*
Tom Paten*
Kola Agbebi*
Dave Lim*

ABSTRACT

Proven plays in North Madura have been identified in the Miocene carbonate and syn-rift Eocene clastic systems. 3D broadband seismic data was acquired in order to obtain higher resolution and deeper imaging of potential prospects and leads within these systems.

Besides improving resolution, penetration, imaging and seismic attributes, broadband data has another major advantage; it allows the low frequencies of the recorded data to drive a more complex velocity model update technique: Full Waveform Inversion (FWI).

Standard traveltimes reflection tomography techniques provide long to mid wavelength velocity updates but generally fail in updating shallow water environments while giving limited resolution in the rest of the velocity model. However, a more accurate velocity model is needed to correct rapid vertical and lateral velocity heterogeneities. Small-scale velocity anomalies in this survey include gas bearing river channels, whereas eroded shallow carbonate platforms present additional challenges related to structural distortions observed on the time domain outputs. Such velocity anomalies must be resolved prior to imaging the deeper section.

FWI operates by minimizing residuals calculated between recorded shot records and modeled shots, within a certain frequency band. An iterative approach was used to update the velocity model starting with low frequencies available from the broadband seismic data. Using the lowest possible frequency data, containing coherent signal, minimizes the risk of cycle skipping thus allowing the FWI update to start from a benign velocity model. The successive passes of FWI introduced details into the velocity model conforming to the geological challenges identified at the beginning of the project.

Combining both broadband data and FWI velocity model building (VMB) is key in correcting for structural distortion and amplitude dimming particularly associated with shallow velocity anomalies. This methodology allowed us to confidently position in depth the potential plays and leads affected by velocity anomalies in the shallower section.

GEOLOGICAL SETTING AND SURVEY OBJECTIVES

The North Madura multi-client surveys are located in East Java, in the back-arc region of Indonesia (Figure 1) and were the first 3D acquisitions over this specific area. Two dual-sensor 3D seismic surveys were acquired over the Central-deep depression and Madura Platform with water depths varying between 60 m and 80 m.

Miocene carbonates and Oligocene-Eocene clastic systems constitute the main proven plays with oil and gas found in surrounding fields (KE38, Ujung and Payang). The Miocene Kujung limestones and Miocene sandstones are the principal geological targets (Fainstein, 1997; Posamentier and Laurin, 2005) while the Ngimbang Formation dating from the Eocene-Oligocene is another potential reservoir (Figure 2).

In this geological setting, a key challenge is the presence of localized shallow river channels and incisions in the carbonate platform creating significant velocity contrast not accurately mapped neither in the initial velocity model nor in the updated velocity model from ray-tracing traveltimes tomography. This leads to large seismic distortions in the deeper section affecting the imaging of the potential targets. Both velocity anomalies are related to the Kalibeng Formation in Late Pliocene. Valley

rivers started incising the formation and soon reached the Ledock Formation, an extensive shallow carbonate platform dated from Early Pliocene that underlies a large part of the surveys. This erosion generated important lateral and vertical velocity contrasts between the river channels and the surrounding sediments, resulting in imaging complexity deeper in the seismic section due to the lack of an accurate velocity model in the shallow section. If the velocity model used during the final migration does not acknowledge these velocity anomalies, structural imaging errors will be introduced in the deeper target levels (Figure 3).

Until now, the identification of new prospects and leads has been limited due to the absence of high quality, modern 3D broadband seismic acquisitions. Indeed, the deeper penetration and higher resolution brought by broadband data (Carlson et al., 2007) enables the detection of additional potential in the proven plays while the integration of Full Waveform Inversion (FWI) (Lailly, 1983; Tarantola, 1984) will address shallow velocity anomalies responsible for the seismic distortions present in the final time and initial depth images.

DATA AND METHOD

Eight dual-sensor streamers towed at 20 m and extending up to 7050 m were deployed with a nominal separation of 150 m. The triple source configuration was set at a depth of 7 m and approximately 2600 km² of data were acquired. Shot gathers with minimal preprocessing were used as input to FWI. Swell noise and mechanical noise attenuation was applied in addition to static corrections. The preprocessed shot gathers input to FWI still contained free-surface energy as all orders of free-surface multiples and source and receiver ghosts were generated by the forward modeling. This modeling uses a ghost-free source wavelet and free-surface boundary at the top of the model.

The acoustic, two-way wave equation with pseudo-analytical extrapolation (Etgen and Brandsberg-Dahl, 2009; Ramos-Martinez et al., 2011) was used to perform the shot modeling. The lowest useable frequency from the broadband seismic data was selected to generate modeled shots and compare them to the recorded ones. For the initial iterations of FWI, shot gathers with a maximum frequency of 5 Hz were selected to keep the modeled and recorded waveforms within half a wave-cycle at this maximum frequency and therefore minimize the possibility of cycle skipping. Transmission energy were used to drive the inversion process and update

the velocity anomalies in this very shallow marine environment. While the velocity for vertical propagation was updated, we kept the anisotropic models delta and epsilon unchanged (Thomsen, 1986; Alkhalifah and Tsvankin, 1995). Starting from a maximum of 5 Hz in the initial passes of FWI, the frequency content was progressively increased up to a maximum of 10 Hz during the velocity model building exercise.

In FWI, data misfit measured between the observed shots and shots modeled using a specific model set (velocity, anisotropy, density, Q) is called objective function or cost function. The bigger the difference calculated between the recorded and modeled shots is, the bigger the cost to solve the system. By finding the minimum of this function, we aim to reproduce similar seismic events at similar locations as the ones in the observed data by deriving high-resolution velocity models. However, the system being highly non-linear multiple minima exist that can describe the minimum of the objective function. We aim to find the minimum of all minima also called the global minimum.

Mathematically, this is formulated as an optimization problem (Beylkin, 1985) and could be directly solved by computing the 2nd order derivative of the objective function (Hessian matrix) with respect to the model parameters. The prohibitive cost of computing and storing the Hessian matrix over large surveys led the industry to seek various approximations for this. Conventional FWI methods use a cross-correlation kernel to compute a gradient, the 1st order derivative of the same objective function. An iterative approach is then implemented to solve the FWI problem (Tarantola, 1984; Mora, 1987) by following the steepest descending solution. However, the velocity update produced can be contaminated by the seismic reflectivity imprint as the inversion is in this case generally dominated by the high wavenumbers of the migration isochron. Based on the work of Whitmore and Crawley (2012), an approach to rely more on the diving wave and back-scattered energy for FWI was developed by combining time and spatial derivative kernels (Ramos-Martinez et al., 2016). The high wavenumbers from the FWI gradient associated with specular reflections are eliminated from the improved velocity kernel while the low wavenumbers are preserved (Figure 4). The remaining low wavenumbers used in the inversion correspond to the diving waves (bananas) and backscattered energy (rabbit ears).

CONVERGENCE AND QUALITY CONTROL (QC)

After each FWI iterations for a specific frequency band, image domain and data domain Quality Controls (QCs) were produced to validate the updated velocity model.

The image domain QC is based on an efficient implementation of Beam Pre-Stack Depth Migration (BPSDM) (Sherwood et al., 2009) to migrate our pre-processed input gathers. Its speed allows repeated migrations at each FWI iteration with stacks and gathers output over the full survey. Structural correlation between seismic image and migration velocity model are illustrated along inlines, crosslines and depth slices. Common Depth Point (CDP) gathers are extracted to estimate the improvement in gather flatness through the updates. Gamma maps (Al-Yahya, 1989) showing the ratio between true geological velocity and current imaging velocities are generated along main interpretations to identify areas of improvement. If available, sonic logs are compared to the updated velocity models.

In addition to the image domain QC, the data domain QC aim to validate the updated models in the shot point domain. This includes crosscorrelation maps that provide an overview of the matching between the forward modeled shots and the observed data. The correlation coefficient and corresponding time-shifts between the modeled and recorded shots used in the inversion are computed for near, mid and far offsets. Figure 5 shows the residual errors before and after the 1st pass of FWI for the near and mid offsets. At the frequency of 5 Hz, the $\frac{1}{2}$ period of the critical cycle skipping is around 100 ms. As the shift values computed prior to the inversion fell below this threshold, this validated the input velocity model for FWI. If the overall time-shift error was larger than the critical value, conventional reflection tomography could be run to generate a more accurate velocity model or the minimum frequency used in the FWI could be lowered if supported by the input seismic data. The global convergence QC is repeated before and after each iteration of FWI. In the example presented, residual errors are minimized after the FWI update allowing further updates using a higher maximum frequency value.

Shot point comparison is an additional QC performed after each pass of FWI. It is a visual QC of the match between the recorded and modeled shots at different offsets. Using the crosscorrelation maps previously introduced, outliers in the QC maps can be analyzed to understand the inversion results. The

direct shot comparison must confirm that with a more accurate velocity model the same complex seismic events as in the observed data are reproduced at the same location and at the same time.

RESULTS AND DISCUSSION

Throughout the VMB exercise, FWI updates captured the velocity required for the imaging process to reduce significantly the moveout seen on the gathers in the shallow to mid-section and minimize the structural distortions apparent on the initial seismic image. Figure 6 shows the initial and final velocity models at shallow depths of 200 m and 570 m. The detailed velocity model generated from FWI conforms to the geology with shallow gas-bearing river channels and incised carbonate platform clearly captured. Lateral resolution too often lacking from conventional reflection tomography was needed to compensate for the near surface velocity anomalies and associated deeper structural uncertainties in the final image. While the shallow river channels extend to a maximum width of 400 m with a distinct velocity variation of around 150 m/s, the deeper eroded carbonate platform shows erosion figures reaching 1000 m with velocity variation of around 325 m/s.

A vertical section in Figure 7 compares the results of the Kirchhoff Pre-Stack Time Migration (KPSTM) stack output and the final TTI Kirchhoff Pre-Stack Depth Migration (KPSDM). The KPSTM volume was converted to depth using its migration velocity while the KPSDM uses the final FWI velocity model. The time migration shows its limitations with obvious sags associated with the river channel and incised carbonate platform anomalies. The structural distortion is only one aspect of the issue visible on the KPSTM as the amplitude and frequency of the associated seismic events are also affected. On the other hand, the high-resolution FWI velocity model used in the KPSDM greatly contributes to improve the continuity, sharpness and amplitude restoration of the seismic events affected by the shallow lateral variations of velocity. While not entirely solved because no Q-compensation was implemented in this project, the KPSDM stack output shows a vast improvement in term of structure and amplitude restoration over the previous KPSTM results.

The quality of the FWI velocity model is primarily responsible for the increase in quality of the final depth product. The low frequency input recorded from the dual-sensor broadband streamers combined with the FWI engine led to a high-resolution velocity model that consequently results in a superior image

of the seismic section. The pushdown artefacts associated with the shallow gas-bearing river channels and incised carbonate platform are minimized improving the seismic events at those locations and deeper in the section.

CONCLUSIONS

We implemented Full Waveform Inversion using a dual-sensor broadband seismic data set acquired offshore North Madura, Indonesia in a shallow marine environment. The resulting high-resolution velocity model conforms to the complex geology observed in the migrated image and captures the velocity anomalies related to gas-bearing channels and an incised carbonate platform. The seismic depth image generated using the FWI velocity model shows minimal structural distortions, better amplitude and frequency content of the seismic events compared to the time migration product. The prospective source and reservoir horizons can then be mapped with more confidence using the improved depth migrated volume.

ACKNOWLEDGMENTS

The authors thank PGS, Migas and SKK Migas for permission to publish the data examples, Suhail Butt, Maz Farouki and Tony Martin for their valuable feedback and Andy Bromley for productive geological discussions.

REFERENCES

- Alkhalifah, T. and Tsvankin, I. [1995], Velocity analysis for transversely isotropic media: *Geophysics*, 60(5), 1550-1566.
- Al-Yahya, K. [1989], Velocity analysis by iterative profile migration, *Geophysics*, 54(6), 718-729.
- Beylkin, G. [1985], Imaging the discontinuities in the inverse scattering problem by inversion of a causal generalized radon transform, *Journal of Mathematical Physics*, 26, 99-108.
- Carlson, D., Long, A., Söllner, W., Tabti, H., Tenghamn, R. and Lunde, N. [2007] Increased resolution and penetration from a towed dual-sensor streamer, *First Break*, 25(12), 71-77.
- Etgen, J. and Brandsberg-Dahl, S. [2009] The pseudoanalytical method: Application of pseudo-Laplacians to acoustic and acoustic anisotropic wave propagation, 79th Annual International Meeting, SEG, Expanded Abstracts, 2552-2555.
- Fainstein, R. [1997] Seismic prospects offshore North Madura, East Java Sea, 57th Annual International Meeting, SEG, Expanded Abstracts, 643-646.
- Lailly, P. [1983] The seismic inverse problem as a sequence of before stack migrations, Conference on Inverse scattering, Theory and Application, Society of Industrial and Applied Mathematics, Expanded Abstracts, 206-220.
- Mora, P.R. [1987] Nonlinear two-dimensional elastic inversion of multi-offset seismic data, *Geophysics*, 52(9), 1211-1228.
- Posamentier, H. W. and Laurin P. [2005] Seismic geomorphology of Oligocene to Miocene carbonate buildups offshore Madura, Indonesia, 75th Annual International Meeting, SEG, Expanded Abstracts, 429-431.
- Ramos-Martinez, J., Crawley, S., Kelly, S., and Tsimelzon, B. [2011], Full-waveform inversion by pseudoanalytic extrapolation, 81st Annual International Meeting, SEG, Expanded Abstracts, 2684-2688.
- Ramos-Martinez, J., Crawley, S., Zou, Z., Valenciano, A. A., Qiu, L. and Chemingui, N. [2016] A robust gradient for long wavelength FWI updates, 78th Conference and Exhibition, EAGE, Extended Abstracts, Th SRS2 03.
- Sherwood, J., Sherwood, K., Tieman, H. and Schleicher, K. [2009] 3D Beam prestack depth migration with examples from around the world, *The Leading Edge*, 28 (9), 1120-1127.
- Tarantola, A. [1984] Inversion of seismic reflection data in the acoustic approximation, *Geophysics*, 49, 1259-1266.
- Thomsen, L. [1986], Weak elastic anisotropy, *Geophysics*, 51(10), 1954-1966.
- Whitmore, D. and Crawley S. [2012], Application of RTM inverse scattering imaging conditions, 82nd Annual International Meeting, SEG, Expanded Abstracts.

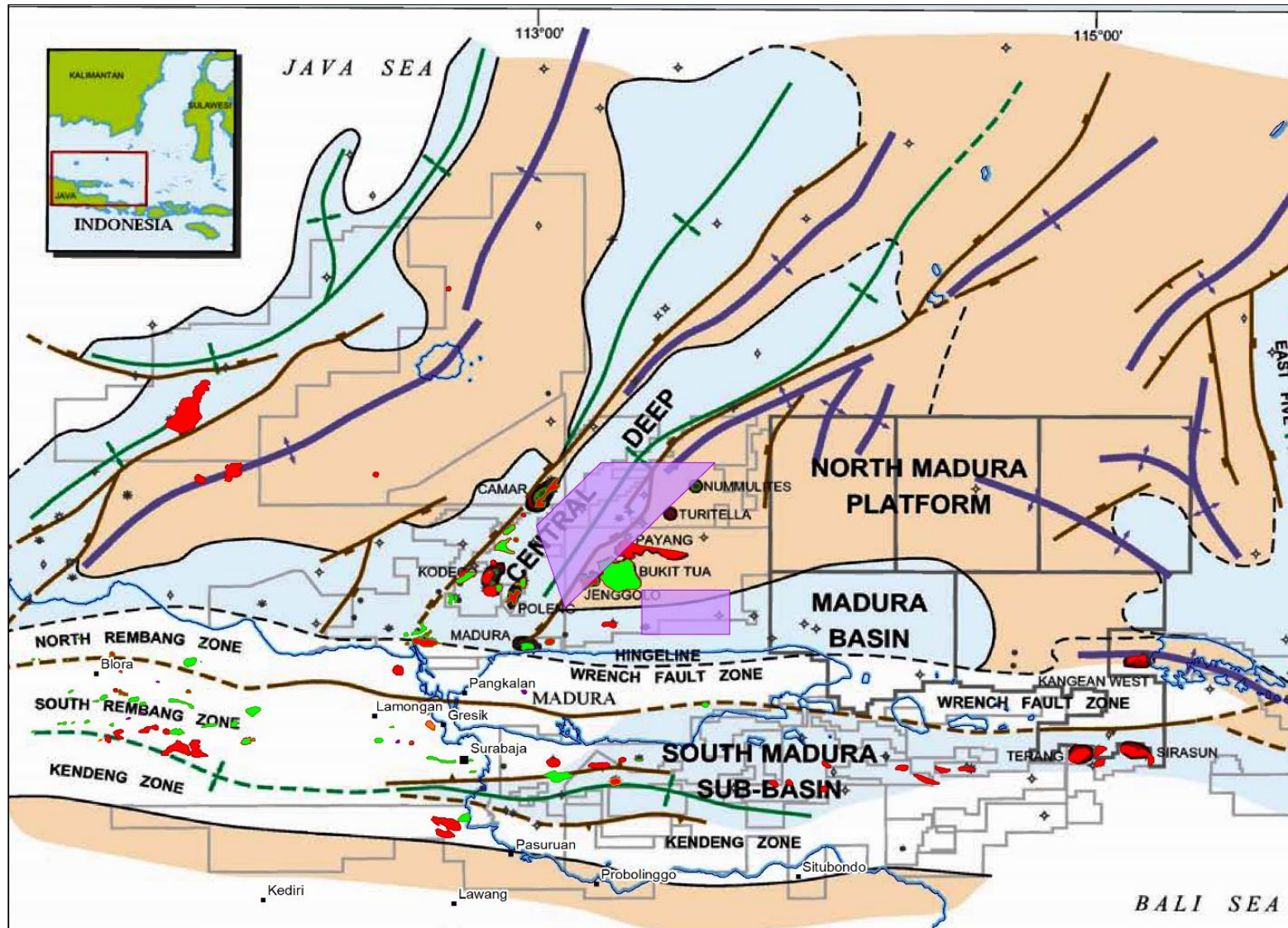


Figure 1 - North Sumatra, East Java location map with newly acquired PGS MC surveys (purple polygons). The main tectonic constraints and structures are indicated on the map (from Johansen K.B., 2003).

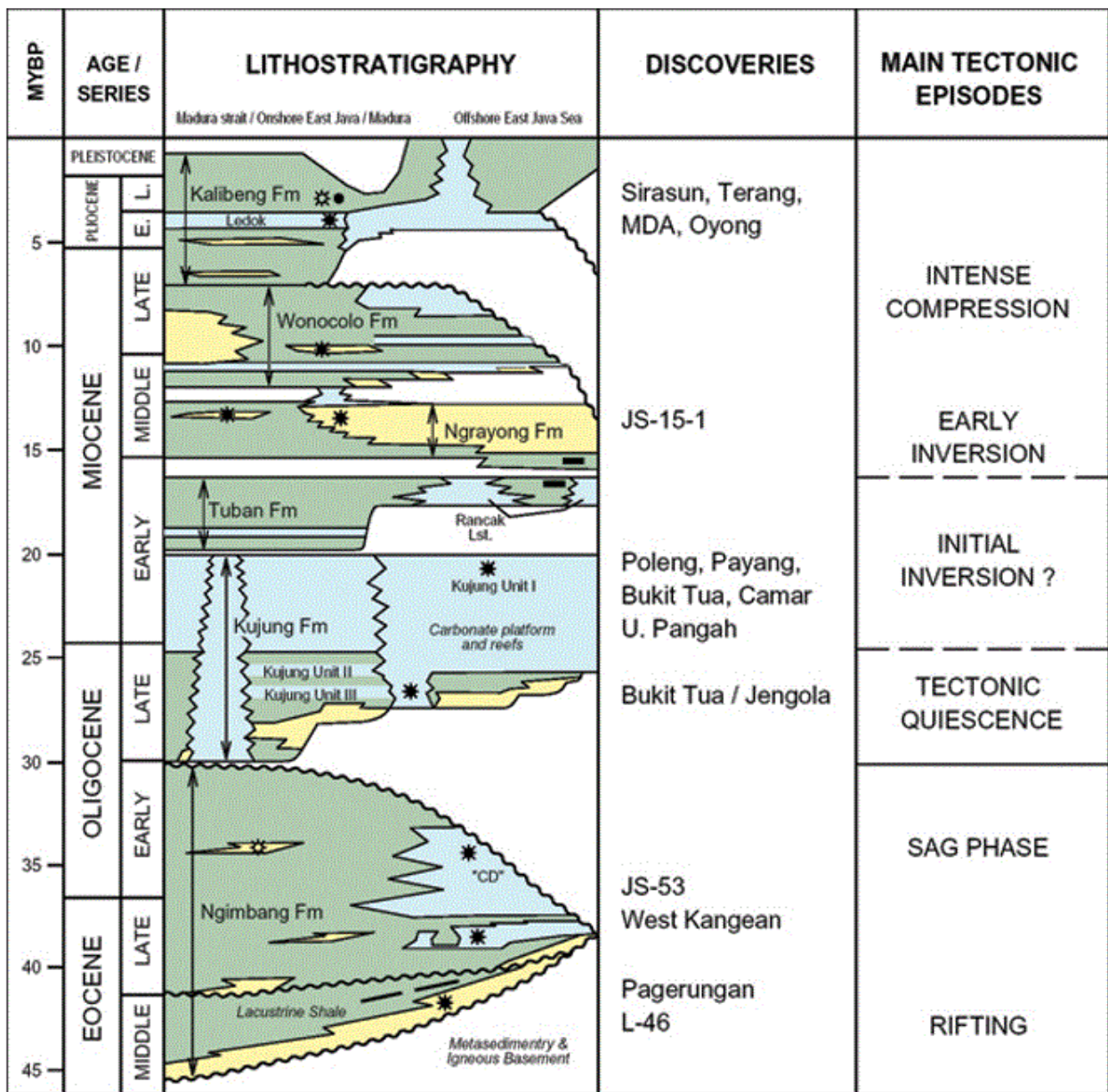


Figure 2 - Tectono-stratigraphy sequence with age of the main series, principal discoveries and tectonic episodes from Eocene until present (from Mudjiono and Pireno, 2002).

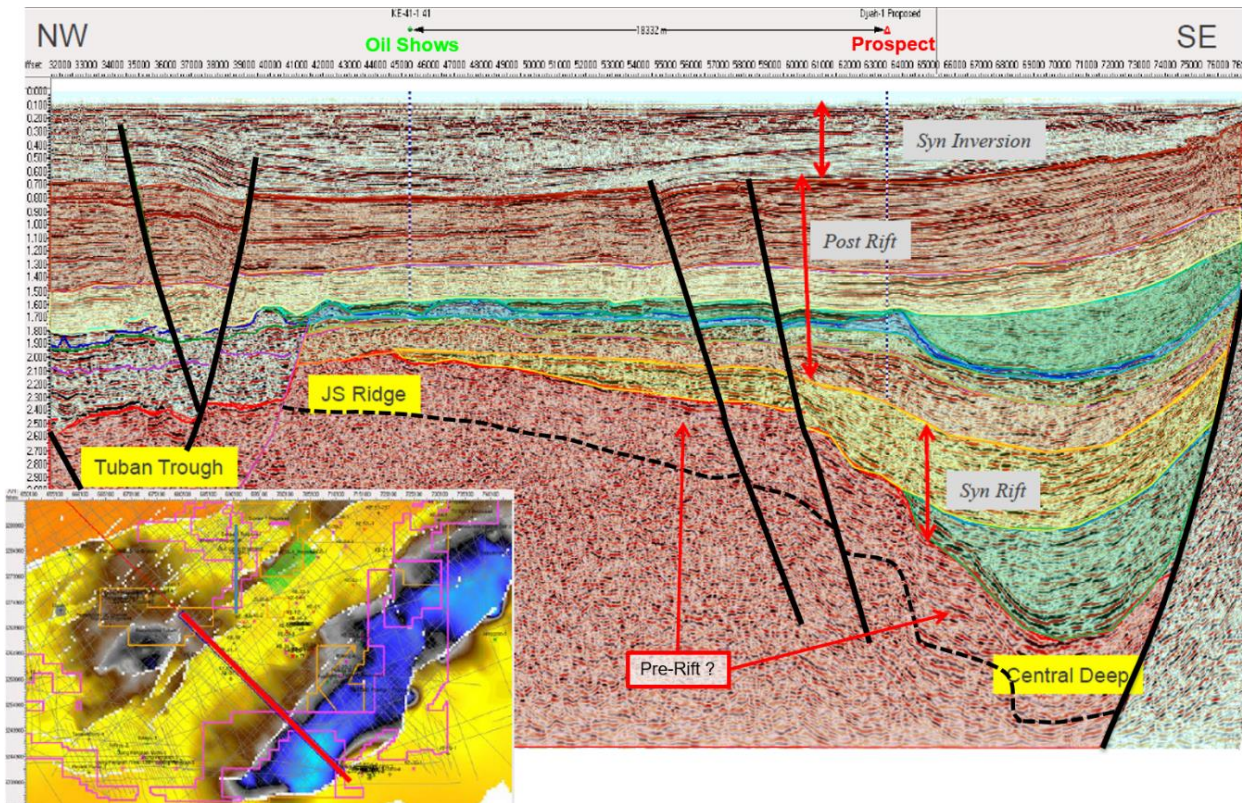


Figure 3 - North Madura seismic cross-section (Basement structural map, modified after Australian Worldwide Exploration 2016) illustrating an interpreted seismic line showing the Central Deep, JS Ridge and part of the Tuban trough. The seismic interpretation displayed shows the main sedimentary packages associated with the major tectonic phases of the Basin: rifting, quiescence and inversion/uplift.

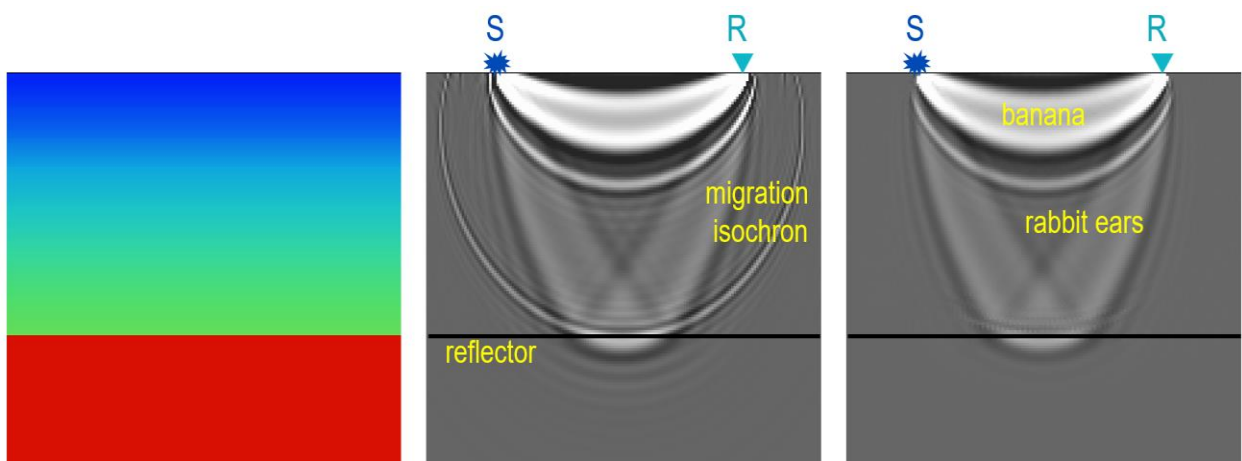


Figure 4 - Simple velocity model (left), conventional kernel (center) and improved velocity kernel (right) showing how the migration isochron (high wave number) is subtracted from the kernel.

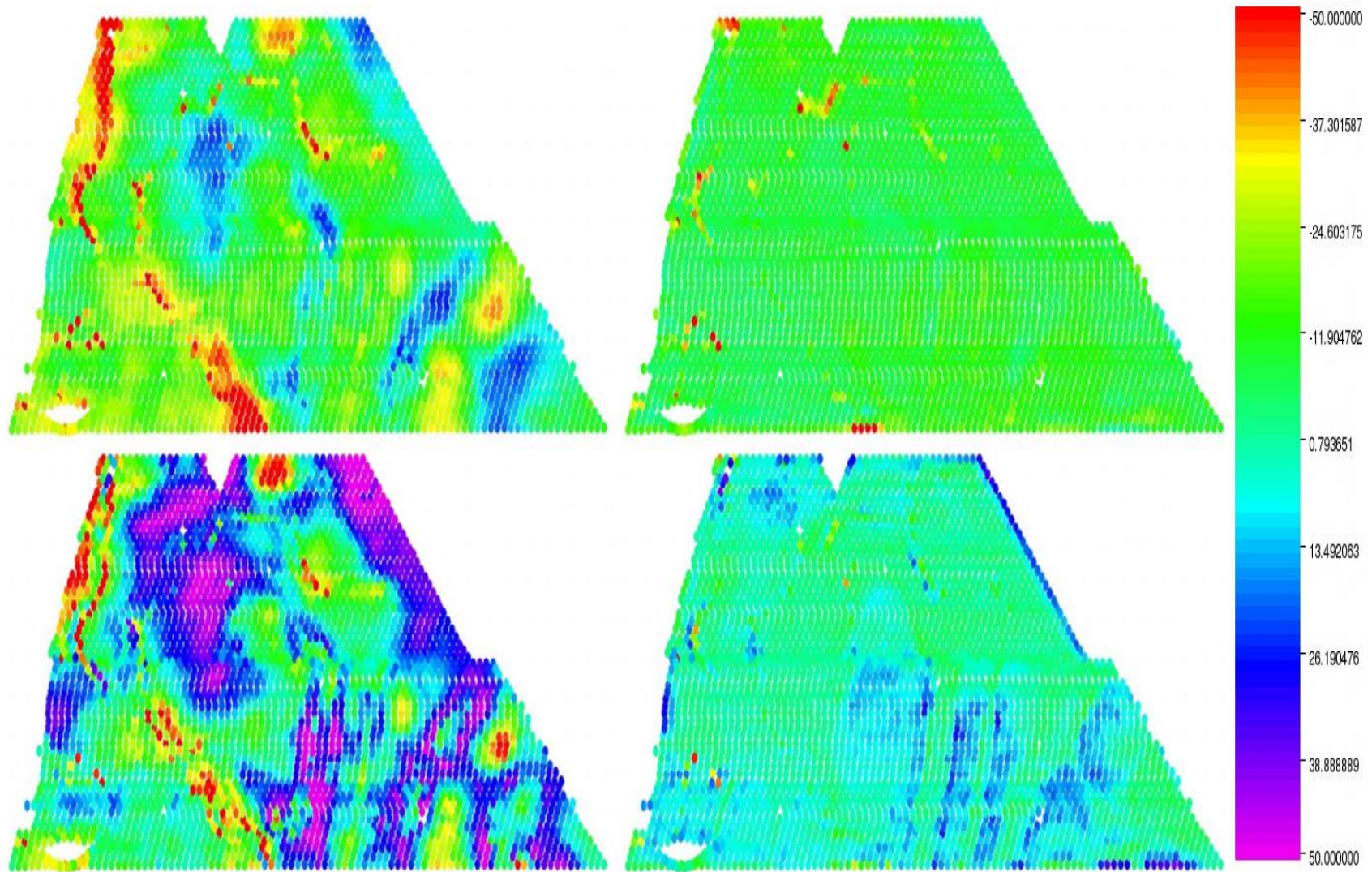


Figure 5 - Data domain QC example showing residual errors (in ms) before (left) and after (right) FWI update for near offsets (top) and mid offsets (bottom). The overall errors have been greatly reduced after the first pass of FWI update (2-5Hz).

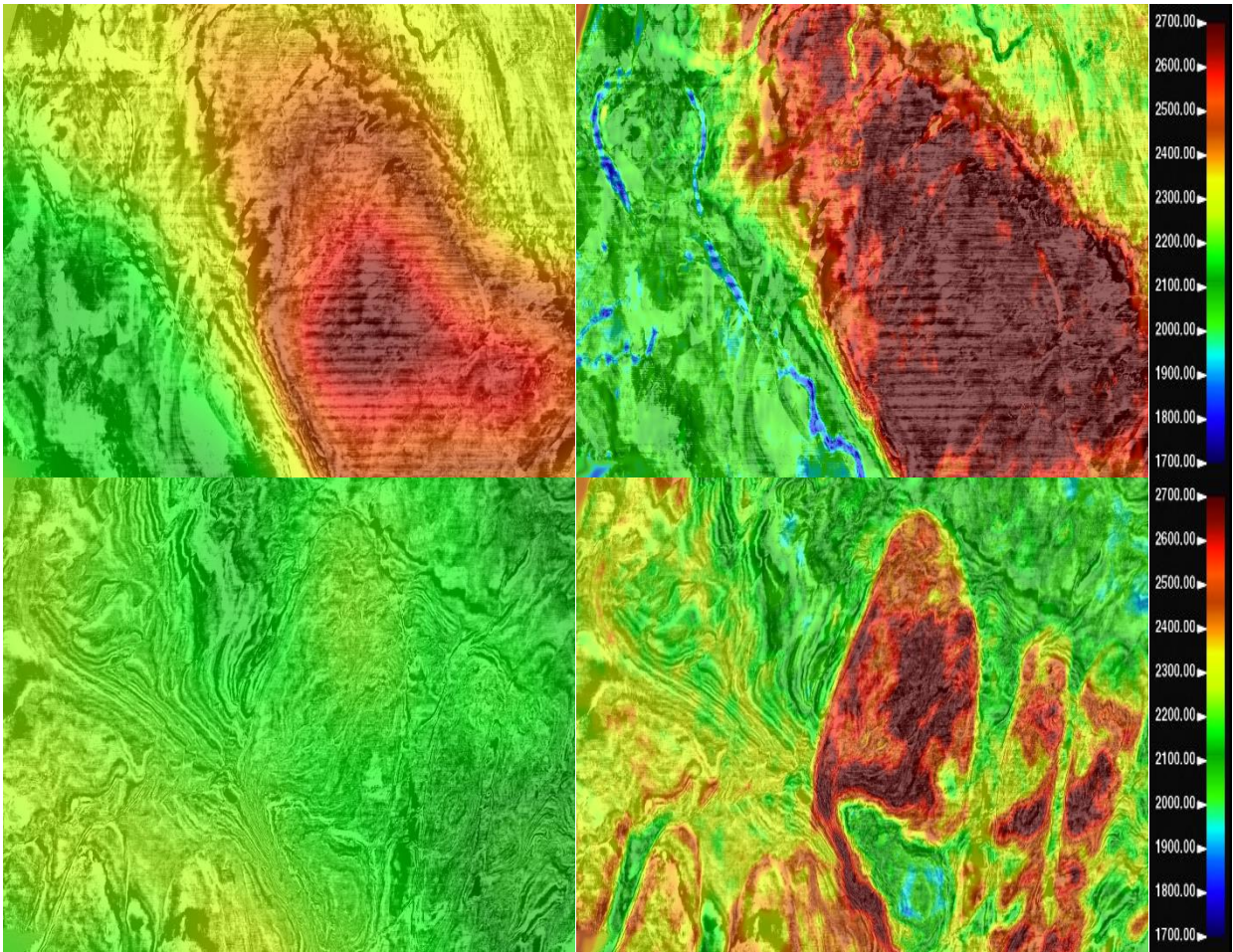


Figure 6 - Initial velocity model (left) at 200 m (top) and 570 m (bottom) and corresponding final velocity model (right). Shallow gas-bearing river channels appear in the FWI update as well as the deeper eroded carbonate platform.

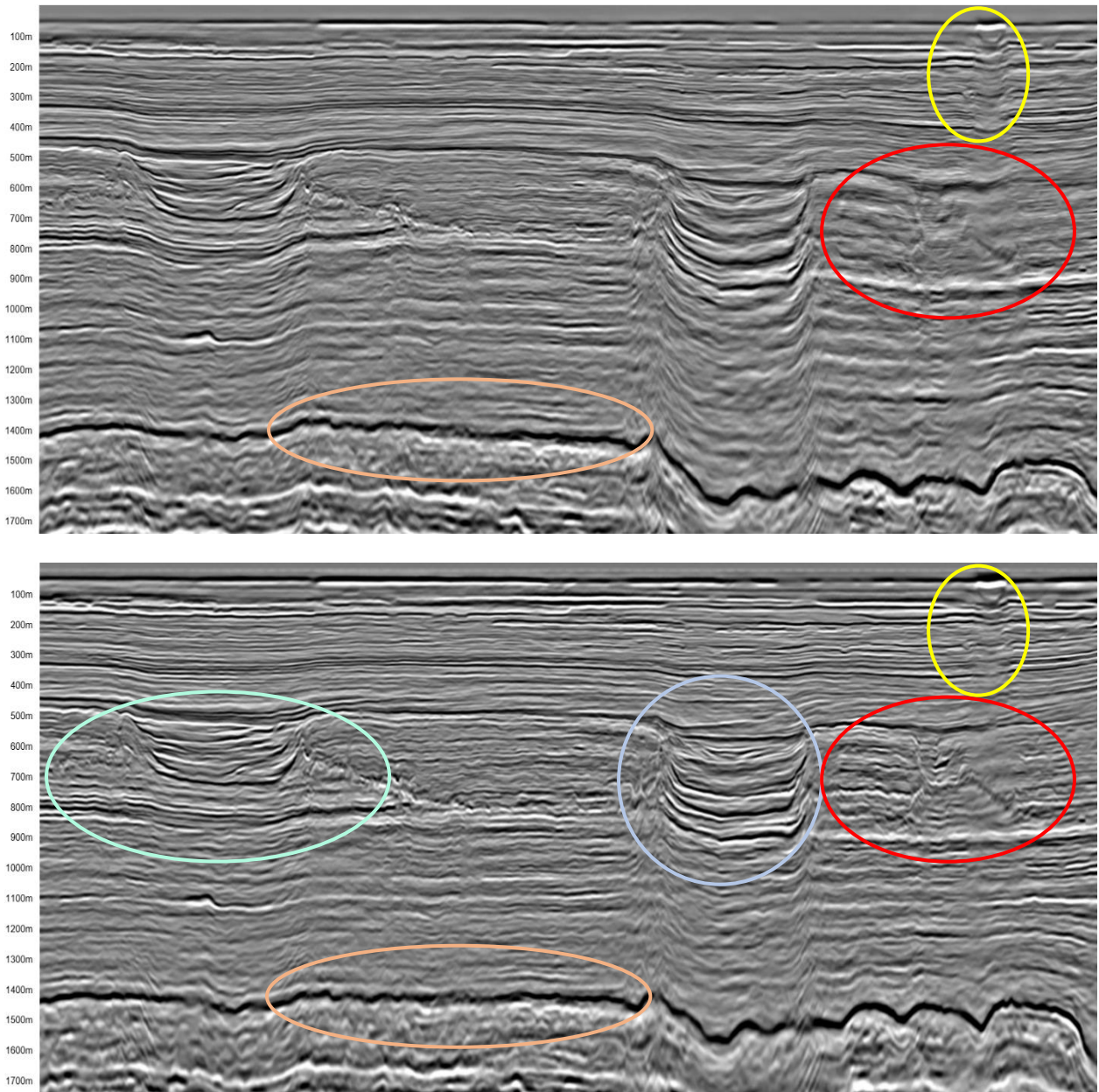


Figure 7 - Final KPSTM converted to depth (top) with its migration velocity model and final KPSDM (bottom) using the velocity model after FWI updates. Areas of improvement in the final image after the FWI updates, reflection tomography passes and final Kirchhoff depth migration are highlighted. Structural distortion visible on the time Kirchhoff output are minimized thanks to the accurate depth velocity model generated from FWI and KPSDM migration scheme used.